Proceedings World Geothermal Congress 2026
Calgary, Canada, June 8 – 11, 2026

Geochemistry of Hot Springs in Bhutan

Finnbogi Óskarsson*[1], Bjarni Richter[1,2], Heimir Hjartarson[3], Tenzin[4], Nima Dorji Tamang[4], Chencho Tshering Namgay[4]

Iceland GeoSurvey (ÍSOR), Kópavogur, Iceland[1], GRÓ Geothermal Training Programme, Kópavogur, Iceland[2], Veitur Utility Company, Reykjavík, Iceland[3], Druk Holding and Investments Ltd., Thimphu, Bhutan[4]

finnbogi.oskarsson@isor.is

Keywords: Geothermal Exploration, Geochemistry, Hot Springs, Bhutan

ABSTRACT

Bhutan's geothermal potential is linked to its position on the boundary of the Indian and Eurasian tectonic plates. This collision results in the formation of numerous hot springs, particularly in the central and northern regions of the country, where the hot springs (*dz.* Tshachu) have been used traditionally for their therapeutic properties. In 2024 the World Bank funded a mission to assess the geothermal potential of Bhutan. As little is known about the hot springs except their location and temperature, the first phase of exploration involved collection and analysis of water samples from all accessible hot springs. 20 samples were collected from nine geothermal areas. In situ temperatures were 27 to 53°C but estimated reservoir temperatures are higher than 100°C for two sites and two other sites have estimated reservoir temperatures above 60°C. Bhutan's geothermal resources, although not fully explored, present opportunities for some electricity generation but mainly direct utilisation. A few hot spring areas show potential for further development, especially if during further exploration the results of geothermometry are confirmed and acceptable permeability is found.

1 INTRODUCTION

Bhutan is a landlocked country in the Eastern Himalayas, between India to the south, west and east and Tibet (China) to the north. The country has a total area of about 38,400 km^2, more than 70% of which are covered by forests, and a population of about 730,000. The topography is quite steep with high mountains and deep valleys carved by glaciers and rivers. The elevation ranges from about 200 m to more than 7500 m. The economy is largely based on agriculture, forestry and tourism and power production is mostly hydroelectric. The areas located at higher elevation, including the capital Thimphu, experience quite cold winters and therefore house heating is essential. At present, urban house heating is mainly by electricity but homes in rural areas are most commonly heated by firewood.

Geothermal energy holds some potential for Bhutan; this is evident by geothermal features such as hot springs, which thus far have mainly been used for bathing. These geothermal features are indicators of subsurface heat, which could be tapped for direct utilisation and possibly power production. They suggest that Bhutan may harness geothermal energy to meet its growing energy demands, thus supporting both economic development and improved quality of life, as well as reducing dependence on imported fossil fuels. However, the full potential of geothermal energy in Bhutan is yet to be realized. The challenges include limited technical expertise, high initial investment costs, including considerable infrastructure cost in many cases, and the need for comprehensive exploration and assessment of the geothermal reservoirs.

In April 2024, the Ministry of Foreign Affairs in Iceland (the Icelandic International Development Agency) and World Bank funded a study intended to review the geothermal potential of Bhutan, to assess on this basis the technical and economical viability of the resources, and to provide recommendations on the next steps to prepare a roadmap for of the development of geothermal resources for electricity generation and direct use in the future. As very little information was available on the geothermal areas of Bhutan, and no information on the chemical composition of geothermal water, a substantial part of the study involved collecting water samples for analysis from the hot springs, in order to assess the likely reservoir temperatures of the geothermal systems and production properties of the geothermal water.

2 OVERVIEW OF GEOLOGICAL AND GEOTHERMAL SETTINGS IN BHUTAN

Bhutan has a complex geological history shaped by the convergence of the Indian and Eurasian tectonic plates. This ongoing collision, which began around 50 million years ago, continues to influence the region's seismic activity, terrain, and landforms. The geological structure of Bhutan can be divided into several key zones, each representing a distinct period of geological formation.

The southern part of Bhutan consists primarily of the Duars Plains, formed by alluvial deposits from rivers. This area is part of the Indo-Gangetic Plain and is composed of sedimentary rocks. Moving northward, the terrain rises dramatically, dominated by the Sub-Himalayan Zone, which is made up of younger sedimentary rocks such as sandstone and shale. These formations were thrust up as part of the collision between the Indian and Eurasian plates, creating the sharp contrasts in Bhutan's landscape. Further north, the Lesser Himalayas dominate, consisting of metamorphic and crystalline rocks, including schists, gneisses, and granite. These rocks were subjected to intense pressure and heat, resulting in their current form. The highest and most rugged terrain, the Greater Himalayas, is composed of crystalline rocks like granite and gneiss. These rocks have been uplifted by the ongoing tectonic forces.

There are 11 known sites with hot springs (*dz.* Tshachu) in Bhutan, particularly in the central and northern regions of the country (Figure 3). Most of them have surface temperatures between 35 and 50°C, and have been used traditionally for their therapeutic properties. Many of the geothermal areas in Bhutan are quite inaccessible, with little or no infrastructure and usually within sparsely populated areas (Dorji et al., 2014).

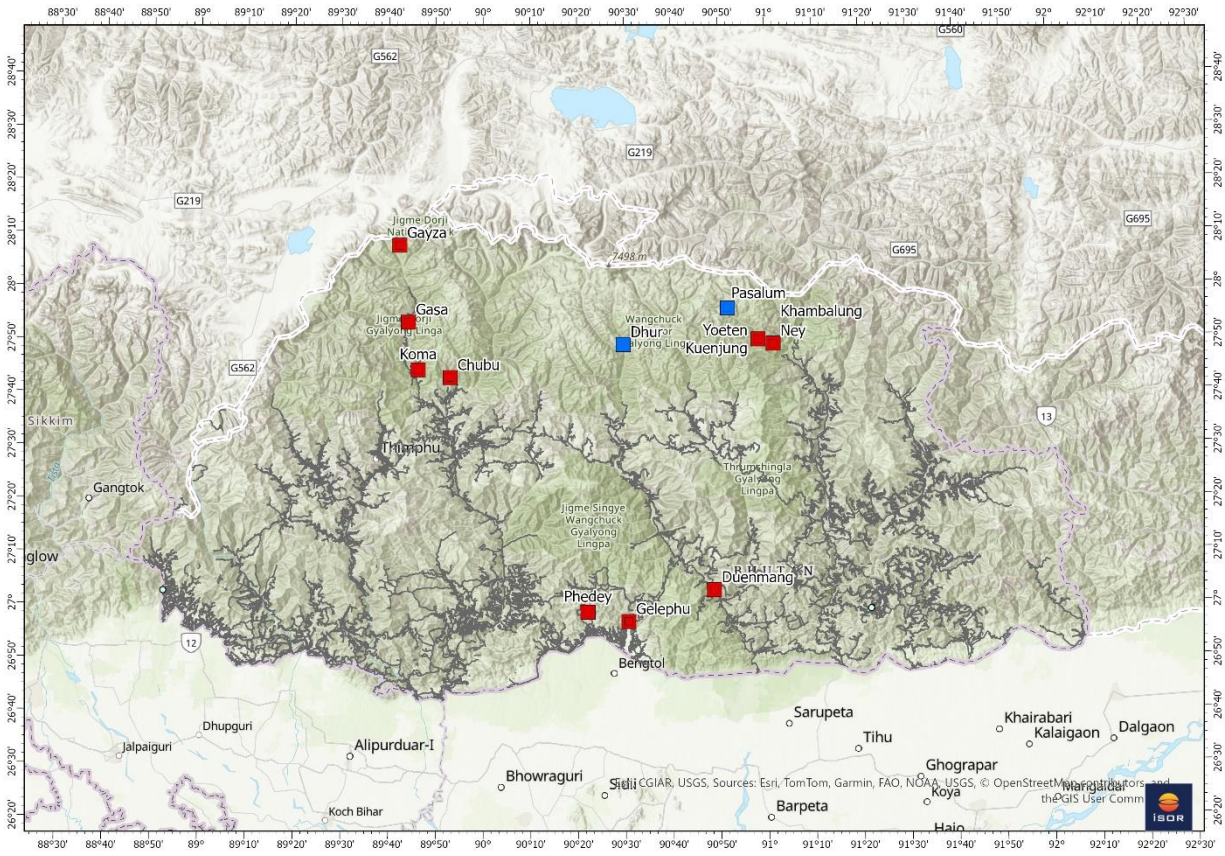


Figure 1. Hot springs (*dz.* Tshachu) in Bhutan. The hot springs marked in red were sampled for this study, but the two marked in blue were inaccessible.

Little published data exists on the chemistry of hot spring waters in Bhutan. An extensive literature search revealed only one article where a few samples from Gasa, Gelephu and Duenmang tshachus are presented (Singh et al., 2004). The results presented below are in reasonable agreement with these results.

3 DESCRIPTION OF HOT SPRING AREAS IN BHUTAN

Chubu Tshachu is located on a riverbank at the foot of a hill in Toedwang, Punakha district. There are three sources with temperatures from 46.6 to 48.8°C, but with a distinct seasonal temperature difference. The hot spring water is channelled through underground pathways for about 30-50 metres, into the bathing facilities. The total flowrate is estimated at 2 L/s. Samples were collected from all three sources.

Duenmang hot spring is located at the bottom of a valley about an hour's walk downhill from the road at about 75 km from Zhemgang. Duenmang Tshachu is located on the right bank of the Mangdechhu river at the base of a steep hill. There are four main sources with temperature ranging from 42.5 to 53.0°C and total discharge is about 1 L/s. All sources were sampled.

The hot spring water at Gasa, Gasa district, is used for bathing in well-developed bathing facilities, but as the water is collected into cisterns and piped from there, the actual outflow of the water could not be observed. According to older site descriptions, before the cisterns were built, the hot water could be observed coming from several sources along an approximately 150 m long linear segment. The estimated flow rate was about 25 L/s in total, and the temperature of the water from the cisterns ranged from 39 to 43°C.

Gayza hot spring is located in the northern part of Laya, Gasa district, which is a two to three-hour long hike from Lungo municipality. Located at an elevation of about 3830 metres, the hot spring sits beautifully within high altitude flora. There are two main sources, one with a temperature of 39.5°C and a flowrate of 0.3 L/s and the other has a temperature of 34.4°C and a flowrate of 0.4 L/s. Samples were collected from these two sources.

Gelephu is located in Sarpang district, near the border to India. There are well-developed bathing facilities at Gelephu. Four different geothermal pools have been built at the site, with measured temperatures from 36.5 to 39.3°C. The location where the hot water emanates from the ground could not be seen. The flowrate into the hottest pool was measured 0.2 L/s but may be slightly higher for other pools. The total flowrate is probably no more than 1 L/s. Samples were collected from the two hottest pools.

Khambalung Ney hot springs are located in Gangzur, Lhuentse district. The hot spring is located at an elevation of 2472 m a.sl. in the middle of a broadleaved forest. Ney Village is one of the closest villages to the hot spring, at a distance of about 7 km. There are three main sources, and the two largest were sampled. The first has a temperature of 39°C and a flowrate of 3 L/s and the second has a temperature of 41.4°C and a flowrate of 2.5 L/s.

Koma Tshachu is located in Goenshari, Punakha district, on the way to the Goenshari Monastery. The waters of Koma Tshachu have been used for balneology. The springs are located at the bottom of a cliff on the banks of the Koma Rongchu River. There are three different sources with temperatures ranging from 33.9 to 40.0°C, which are stable throughout the year. The water has a sulphurous odour, and the total flowrate is estimated at about 1 L/s. Samples were collected from all three sources.

Phedey hot spring is located in Dekiling, Sarpang district. The hot spring is located on the bank of Tato Pani Khola river, at an elevation of 687 m a.sl. and the hot water flows out through fractured rock. Menchuthang Village is one of the closest villages to the hot spring, at a distance of about 5-6 km. There are two springs with temperatures 27.3 and 28.8°C and flowrates 0.2 L/s and 0.1 L/s. Samples were collected from both springs.

Yoeten Kuenjung hot spring is located in Gangzur, Lhuentse district. The hot spring is located at an elevation of 2761 m a.sl. in the middle of a broadleaved forest, on the bank of the river Ya La Gang. There is about two to three days walk to the hot spring from Ney village, which has around 70 households. There is only one source, with water flowing from under rocks. The temperature is 39°C but the flowrate could not be determined.

4 CHEMICAL COMPOSITION OF HOT SPRINGS IN BHUTAN

4.1 Sample collection

During the site visit to Bhutan in May 2024, water samples for chemical analysis were collected from two of the most accessible geothermal areas, Gasa and Gelephu. Following the site visit, samples were collected from seven more geothermal areas from mid May until the end of November 2024. A total of 20 samples were collected from 9 geothermal fields for this study: Chubu, Duenmang, Gasa, Gayza, Gelephu, Koma, Khambalung Ney, Phedey and Yoeten Kuenjung. Two of the proposed sampling sites, Dhur and Passanglum, were not accessible for sampling during this study due to monsoon rains and associated risks.

Upon sample collection, the pH, electrical conductivity and temperature of the water was measured, and the flow rate estimated. Each hot spring sample was collected into four bottles; raw untreated samples into two 60 mL amber glass bottles and one 200 mL HDPE bottle for analysis of dissolved inorganic carbon, anions, TDS and stable water isotopes, and a filtered sample (0.2 µm nylon syringe filter) for cation and trace element analysis into a 100 mL HDPE bottle, which was then acidified (1% v/v) with purified concentrated nitric acid (HNO_3).

At the laboratory, pH and conductivity at room temperature were determined using appropriate electrodes; the concentration of dissolved inorganic carbon (DIC; reported as CO_2) was determined by modified alkalinity

titration and back-titration; the concentrations of anions (F^-, Cl^-, Br^-, NO_3^-, SO_4^{2-}) were analysed by suppressed ion chromatography (IC); the concentrations of SiO_2, B and main metals (including Na, K, Ca, Mg) were analysed by ICP-OES; and the total amount of dissolved solids (TDS) was determined by gravimetry. Determination of stable isotope ratios ($^2H/^1H$ and $^{18}O/^{16}O$) was carried out by IRMS at the University of Iceland Institute of Earth Sciences. Trace elements were determined using ICP-MS at ALS Laboratories in Luleå, Sweden.

4.2 Geothermal water characteristics

Results for representative samples from all fields are given in Table A1 in the Appendix. The samples shown in the table are generally the hottest sample collected from each field, however all samples are shown in the figures. The pH is reported both as measured in situ during sampling and in the ÍSOR laboratory upon arrival. The results span some range in terms of composition, with pH ranging from 6.66 to 9.95 and total dissolved solids (TDS) from 111 to 5420 mg/L. A few samples, particularly those from Gasa, Gayza and Chubu hot springs have elevated concentrations of silica (> 50 mg/L) suggesting higher temperatures at depth.

It is worth noting that fluoride concentrations are quite high in a number of samples, particularly those from Koma (17 mg/L), Chubu (14 mg/L), Gayza (7.7 mg/L), Phedey (6.6 mg/L), Yoeten Kuenjung (5.2 mg/L), Gasa (4.2 mg/L) and Khambalung Ney (2.9 mg/L). These concentrations are above the maximum fluoride concentration for potable water recommended by the World Health Organization (1.5 mg/L; WHO, 2022), therefore the water is not considered fit for consumption. The concentrations of arsenic, boron and manganese in some samples also exceed the maximum concentrations for potable water (WHO, 2022). Therefore, drinking the water is not advisable, at least not in large quantities. There are however no restrictions on the use of the water for bathing.

Figure 2 shows the cation (Na-K-Mg) composition of the water plotted on the ternary diagram suggested by Giggenbach (1988). Also shown are Giggenbach's calibrations for the Na/K and K/Mg geothermometers, the line where the two agree, suggesting that the water is in equilibrium with the minerals relevant to the two geothermometers, and the areas of partial equilibrium and no equilibrium. The river water plots right at the magnesium apex, as would be expected for cold water, and the samples from most hot springs are plotted in the partial equilibrium zone, suggesting some reaction with rock but not full equilibrium. When full equilibrium is not obtained, the K/Mg geothermometer is more likely to give a good temperature estimate rather than the Na/K geothermometer and this suggests a temperature close to 130°C for Gasa, close to 100°C for Phedey and Gayza, but less than 100°C for the remaining samples.

Figure 3 shows the concentration of silica in the samples plotted against the water temperature (left) and chloride concentration (right). Also shown in the left panel are the solubility curves for three silica mineral phases: amorphous silica (grey), chalcedony (blue) and quartz (black). The left part of the figure shows that the samples from Gelephu and Duenmang are at equilibrium with chalcedony at the discharge temperatures, suggesting that they are close to the expected reservoir temperature, whereas the samples from other fields suggest that they come from a reservoir that is hotter than the temperature measured on surface – particularly Gasa and Gayza for which silica concentrations are more than 50 mg/L higher than expected. This is in good agreement with the figure in the right panel which shows that for most fields there is a general increase in silica concentration with increasing chloride concentration which probably reflects a greater extent of water-rock interaction. Gelephu and Duenmang are notable exceptions, as silica appears to decrease with increasing chloride concentration, suggesting that the hot water is less saline than the surrounding groundwater.

Figure 4 shows the chloride to boron ratio (by mass) in the samples plotted against the chloride concentration (note that both axes are logarithmic). Also shown is the composition of seawater, rainwater (assuming 2 mg/L of chloride) and lines which represent the progressive reaction of rainwater with granite (assumed to have a Cl/B ratio of 23; brown line) and mixing with seawater (dark blue line). Assuming that all water is in contact with granite is an oversimplification, but the trend would be quite similar for other rock compositions even though the asymptotic value would be different. All the hot spring samples have quite low Cl/B values, ranging from 21 to 60, suggesting significant reaction with rock. The samples from Gayza and Gasa are at the lower end of the range, but the highest ratio is for the sample from Khambalung Ney. Again, the sample from Gasa shows the greatest extent of water-rock interaction, followed by Gayza, Chubu, Koma and Phedey.

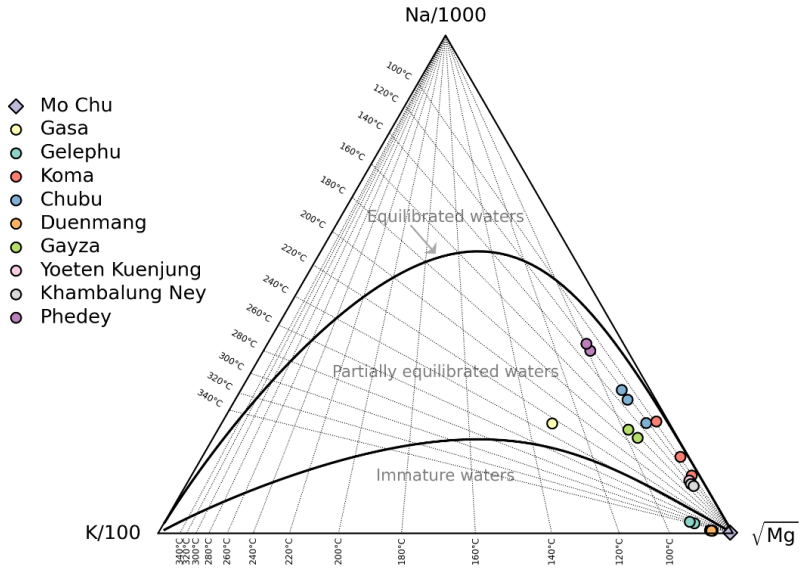


Figure 2. Na-K-Mg ternary diagram for water samples from Bhutan.

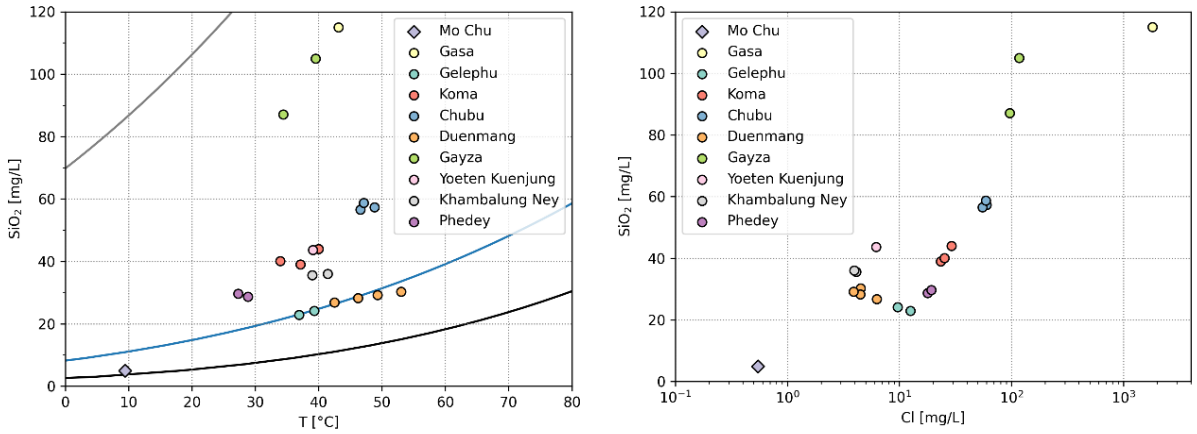


Figure 3. Silica concentration plotted against discharge temperature (left) and chloride concentration (right). In the left panel, the solid lines represent the solubilities of three silica mineral phases: amorphous silica (grey), chalcedony (blue) and quartz (black).

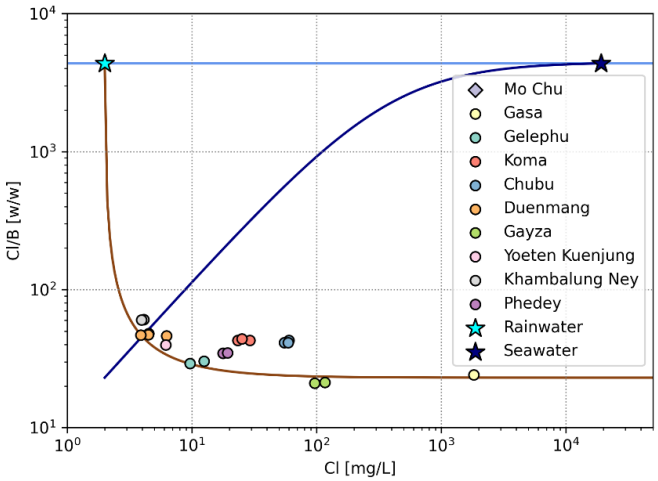


Figure 4. The mass ratio of chloride to boron against chloride concentration. The composition of rainwater and seawater is also shown. The brown line represents a reaction between the water and rock (assuming a Cl/B ratio of 23 for granite) whereas the dark blue line represents mixing with seawater.

The relationship between oxygen and hydrogen isotope values is shown in the left panel of Figure 5, along with the global meteoric water line as defined by Craig (1961) and the local meteoric water line for Nepal (Jeelani and Deshpande, 2017) – since no such data was found for Bhutan. The figure shows that there is little difference between the local and global isotopic trends in precipitation and that most of the samples follow the trendlines, suggesting that their origin is meteoric. Only the samples from Gasa and Koma show a slight shift towards less negative oxygen isotope values, which could be an indication of oxygen isotope exchange with rock, probably at elevated temperatures.

The right panel of Figure 5 shows the relationship between the deuterium content of the water and its elevation. The lowest deuterium values by far are those from the Gayza hot springs (δD ≈ -120‰, relative to V-SMOW), collected at about 3900 m a.sl. and may originate from even higher altitude. On the other end of the range are the waters at Gelephu, Duenmang and Phedey, collected at 380, 250 and 690 m elevation, respectively. The only river sample collected for reference is from Mo Chu river next to the Gasa hot springs, at about 2100 m a.sl. Based on the deuterium content, the water that feeds the hot springs (δD ≈ -92‰) is precipitation from much higher (~2000 m) altitude than the river water (δD ≈ -65‰).

There is little available data on stable water isotopes in precipitation in Bhutan, but studies from other parts of the Himalayas indicate that the oxygen-18 and deuterium content of precipitation decreases by about 0.2‰ and 1.6‰ respectively, per 100 m increase in altitude (Jeelani et al., 2017; Acharya et al., 2020). The trend in deuterium with altitude is shown as a straight line in Figure 5, assuming that the water from Mo Chu river is precipitation from 2200 m elevation. Although it is unlikely that one sample from a river is good enough to define this line, since annual fluctuations in isotopic composition of river waters in the Himalayas are very large (e.g. Tshering et al., 2020), the slope should be fairly well defined. Therefore, to better visualise the trend, a dashed line with the same slope but shifted by a somewhat arbitrary -15‰ is also shown in the figure. A comparison of the deuterium values and the shifted trendline suggests that the hot spring waters at Chubu, Koma, Gasa, Gayza and Duenmang may have fallen as precipitation at 500-2000 m higher altitude than the springs, again indicating longer contact time with the host rock.

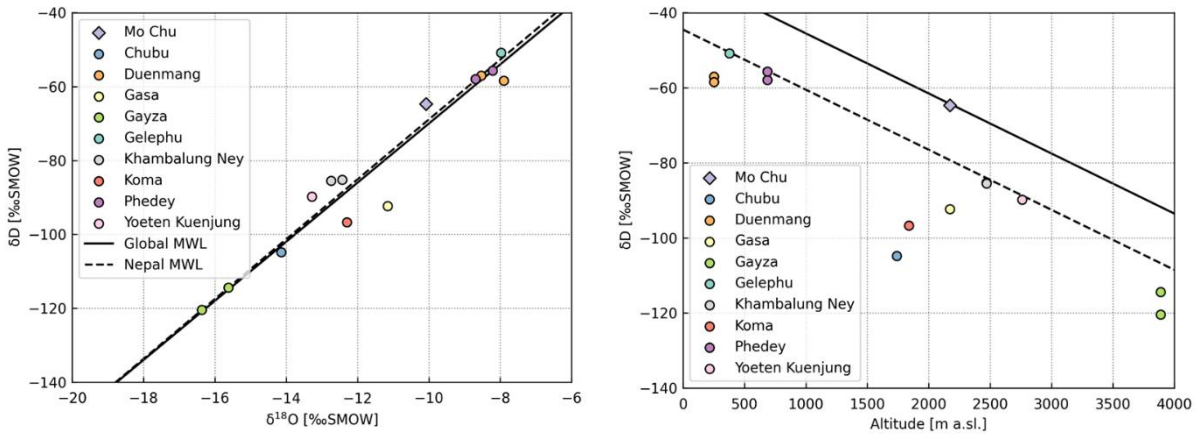


Figure 5. Deuterium content of the samples, plotted against oxygen isotope values (left) and sample altitude (right). The lines in the left panel represent the global meteoric water line (Craig, 1961) and the meteoric line for Nepal (Jeelani and Deshpande, 2017). The solid line in the right panel shows the altitude trend for deuterium in precipitation (-1.6‰ per 100 m), drawn through the sample from the Mo Chu river, and the dashed line is the same trendline shifted by -15‰.

4.3 Geothermometry

One of the main goals of geochemical exploration is to assess the reservoir temperature of the potential geothermal system. Such interpretation assumes that some chemical equilibrium exists between dissolved species in the water and mineral phases in the rock. This assumption does not always hold, particularly when water temperatures are low and the chemical reactions involved are slow. Different calibrations of geothermometers exist and they have different strengths and weaknesses.

Table 1 shows results for seven different solute geothermometers and the measured temperature for the hot spring samples. Two silica geothermometers are used, assuming equilibrium with chalcedony (Fournier, 1977) and quartz (Fournier and Potter, 1982), and five cation geothermometers; namely Na-K-Ca (Fournier and

Truesdell, 1973), Na/K (Arnórsson et al., 1983), K/Mg (Giggenbach, 1988), Na/Li (Kharaka and Mariner, 1989) and Li/Mg (Kharaka and Mariner, 1989).

The results in Table 1 indicate that generally there is good agreement between the silica (chalcedony) geothermometers and those that include magnesium whereas the geothermometers that are based on sodium concentrations give much higher temperatures. This is quite common at temperatures lower than 100°C and is consistent with the interpretation of Figure 2. Therefore, there is more reason to put faith in the results from the silica and magnesium based geothermometers than those that use sodium ratios – particularly since many of the waters appear to be immature or only in partial equilibrium according to the classification shown in Figure 2.

Table 1. Measured sample temperature and geothermometry temperatures for representative hot spring samples from Bhutan. All temperatures are in °C.

Sample	Location	T_{sample}	T_{chal}	T_{qtz}	$T_{Na-K-Ca}$	$T_{Na/K}$	$T_{K/Mg}$	$T_{Na/Li}$	$T_{Li/Mg}$
20248011	Chubu 1	48.8	77	107	112	68	87	117	83
20248013	Duenmang 2	53.0	48	80	227	474	72	175	24
20248008	Gasa	43.1	119	145	240	187	133	226	142
20248031	Gayza 1	39.5	113	140	117	113	98	175	108
20248006	Gelephu 1	39.3	39	71	210	329	83	164	42
20248035	Khambalung Ney 2	41.4	44	76	97	80	61	134	62
20248010	Koma 1	40.0	58	90	84	36	65	101	67
20248036	Phedey 1	28.8	27	59	92	67	100	86	76
20248033	Yoeten Kuenjung	39.1	32	64	93	78	63	166	80

For Chubu, the K/Mg, Li/Mg and chalcedony geothermometers are in rather good agreement at a temperature range of 74-88°C, suggesting that water with higher temperature than the discharge temperature can be found at depth. The water composition suggests considerable equilibration with rock which suggest that the application of geothermometry is justified.

For Duenmang, the chalcedony geothermometer gives values similar to the discharge temperatures, suggesting that it is unlikely that much hotter water can be found at depth. The samples fall within the immature waters field in Figure 2, suggesting that cation geothermometry is not reliable. Most likely, the water is not hotter at depth than at surface.

For Gasa, the K/Mg, Li/Mg and silica geothermometers give values ranging from 119°C (chalcedony) to 145°C (quartz). Given the evidence of water-rock interaction observed for this sample, e.g. low Cl/B ratio and a significant oxygen isotope shift, these geothermometry results are quite credible and are considered likely to reflect the reservoir temperature of the geothermal system. Therefore, it is expected that temperatures in excess of 120°C may be found by drilling into a potential reservoir.

The samples from Gayza show quite good agreement between the geothermometers based on chalcedony, Na-K-Ca, Na/K and Li/Mg, ranging from 108 to 117°C for the hotter sample (Gayza 1), with the K/Mg geothermometer closely following at 98°C. The samples show some signs of water-rock interaction, including high concentrations of silica, boron, arsenic and fluoride, and therefore it may be considered likely that the reservoir temperature at Gayza is on the order of 110°C.

For Gelephu, there is excellent agreement between the measured temperature, the chalcedony temperature and the Li/Mg temperature. As for Duenmang, the Gelephu waters fall into the immature waters field in Figure 2. This suggests that the reservoir temperature at Gelephu is not much higher than the measured temperature at the surface.

Similarly, the samples from Khambalung Ney, show excellent agreement between the measured temperature and the chalcedony temperature. These samples fall very close to the Mg corner of Figure 2 so cation geothermometry is dubious at best. Therefore, the reservoir temperature at Khambalung Ney is unlikely to be higher than the discharge temperature.

For Koma, the K/Mg, Li/Mg and chalcedony geothermometry results for the hottest sample are in fairly good agreement at a temperature range of 58-67°C suggesting waters at least 20°C hotter at depth than at the surface.

Óskarsson et al.

The samples from Phedey have very low silica concentrations, similar to the samples from Duenmang and Gelephu, and chalcedony geothermometry suggests temperatures similar to the discharge temperatures. However, the samples plot relatively high in the partial equilibrium field of Figure 2 with Giggenbach's (1988) cation geothermometers suggesting temperatures between 60 and 100°C, which also matches the quartz temperature. On the other hand, the Na/K temperature in Table 1 (~65°C) is calculated using the geothermometer of Arnórsson et al. (1983) which tends to be more reliable in low temperature waters. As the local mineralogy is not known, the possibility of temperatures close to or above 60°C at depth cannot be excluded. The discrepancy between the Na/K geothermometers of Arnórsson et al. and Giggenbach (and several others that have been published and also do not agree, e.g. that of Fournier (1979) which gives about 100°C for Phedey) demonstrates well the approximate nature of cation geothermometry in general.

The sample from Yoeten Kuenjung falls close to the Mg corner of Figure 2 so cation geothermometry is probably not justified. The silica concentration is elevated, although not particularly high, but this could be partly due to the high pH of the water. The high pH also causes increased uncertainty in the use of silica geothermometers. The chalcedony geothermometer yields a temperature slightly lower than the discharge temperature, so it is unlikely that hotter water can be found by drilling.

4.4 Production properties

Regarding potential utilisation, the main risks posed by the chemistry of the thermal fluids are typically corrosion and scale formation. The risks would have to be assessed with respect to the type of utilisation envisaged at each site. The only water that is likely to be corrosive due to high salinity is the water at Gasa (1820 mg/L Cl), but the concentration of free carbonic acid (H_2CO_3), which can also cause corrosion, is high both in Gasa and Gayza. Generally, corrosion can be mitigated by careful material selection and/or an inhibitor system.

As for scaling, the most common scales formed in low-temperature utilisation are calcite ($CaCO_3$) which typically forms during fluid degassing and/or mixing, and amorphous silica (SiO_2) which precipitates from silica-rich solutions when they cool below the saturation limit of amorphous silica (about 120 mg/L at 25°C). None of the waters sampled in Bhutan are supersaturated with respect to amorphous silica so there is little risk of silica deposition during utilisation of the fluids. Some of the waters, including those at Gasa, Phedey and Duenmang are supersaturated with respect to calcite, suggesting that calcite may precipitate during production. Calcite precipitation can often be mitigated by pH modification or injection of a commercial scaling inhibitor.

5 CONCLUSIONS AND RECOMMENDATIONS

Water samples from nine different geothermal areas in Bhutan have been analysed. The results show different geochemical characteristics suggesting different formation processes and, in two cases, indications of reservoir temperatures in excess of 100°C. The most promising site is Gasa which has the highest flowrates and may also have a reservoir temperature high enough for binary power generation. The hot effluent from such a power plant has potential for cascaded use in different applications, such as greenhouse growing, drying, heating, fish farming etc. A few other hot spring areas (Gayza, Chubu, Koma) show potential for further development, especially if resource temperatures at depth confirm what the geochemical results indicate, as well as finding good permeability. Most of the areas show little or no indication that hotter water can be found at depth.

Now that this study has identified the most promising sites for further geothermal exploration, a phased approach is recommended, starting with a detailed geological and structural survey, trying to identify the main structures hosting the upflow of the geothermal fluids and how the surface manifestations relate to these structures. Due to difficult topography in most cases, the need for remote sensing techniques will be essential. The immediate next step should focus on investigating the potential utilisation for each of the most promising sites, i.e. what kind of utilisation can be developed and what is feasible, taking into account potential flowrates, potential temperatures, chemical composition of the fluids, infrastructure needed and positive impact on the local community as well as regionally.

Geothermal energy can offer Bhutan a reliable and sustainable energy source, within several local areas. Beyond energy production, geothermal development holds substantial socio-economic benefits. It could generate local employment, support sustainable agricultural practices, and contribute to Bhutan's goals of reducing carbon emissions and promoting renewable energy. The development of a geothermal resource roadmap, based on the findings of this study, will guide the country towards strategic geothermal development. Continued data collection, exploration, and engagement with key stakeholders could be essential to realize Bhutan's geothermal potential.

Acknowledgements

The authors gratefully acknowledge the World Bank and the Icelandic Ministry of Foreign Affairs (ICEIDA) for funding the study, including site visits and chemical analyses, Druk Holding and Investments (DHI) and the Government of Bhutan for facilitating sample collection and the laboratories of Iceland GeoSurvey (ÍSOR) and the University of Iceland Institute of Earth Sciences for analysing the samples. Thanks to Gunnlaugur M. Einarsson (ÍSOR) for preparing maps.

REFERENCES

Acharya, S., Yang, X., Yao, T and Shrestha, D.: Stable isotopes of precipitation in Nepal Himalaya highlight the topographic influence on moisture transport. *Quaternary International,* **565**, (2020), 22-30.

Arnórsson, S., Gunnlaugsson, E. and Svavarsson, H.: The chemistry of geothermal waters in Iceland. III. Chemical geothermometry in geothermal investigations. *Geochimica et Cosmochimica Acta,* **47***,* (1983), 567-577.

Arnórsson, S., Bjarnason, J.Ö., Giroud, N., Gunnarsson, I. and Stefánsson, A.: Sampling and analysis of geothermal fluids. *Geofluids,* **6***,* (2006), 203-216.

Craig, H.: Isotopic variations in meteoric waters. *Science,* **133***, (1961),* 1702-1703.

Dorji, T., Wangdi, N. and Wangdi, K.: *Hotsprings and Mineral Springs of Bhutan*. Ugyen Wangchuck Institute for Conservation and Environment. Lamai Gompa: Bumthang. UWICE Press, (2014).

Fournier, R.O.: Chemical geothermometers and mixing models for geothermal systems. *Geothermics,* **5***,* (1977), 41-50.

Fournier, R.O. and Potter, R.W.: A revised and expanded silica (quartz) geothermometer. *GRC Bulletin*, **11 (10)**, (1982), 3–12.

Fournier, R.O. and Truesdell, A.: An empirical Na-K-Ca geothermometer for natural waters. *Geochimica et Cosmochimica Acta,* **37***,* (1973), 1255-1275.

Giggenbach, W.F.: Geothermal solute equilibria. *Geochimica et Cosmochimica Acta,* **52***,* (1988), 2749-2765.

Jeelani, G. and Deshpande, R.D.: Isotope fingerprinting of precipitation associated with western disturbances and Indian summer monsoons across the Himalayas. *Journal of Earth System Science,* **126***,* (2017), *10*8.

Jeelani, G., Shah, R.A., Fryar, A.E., Deshpande, R.D., Mukherjee, A. and Perrin, J.:. Hydrological processes in glacierized high-altitude basins of the western Himalayas. *Hydrogeology Journal,* **26***,* (2017), 615-628.

Kharaka, Y.K. and Mariner, R.H.: Chemical geothermometers and their application to formation waters from sedimentary basins. In: Naeser, N.D. and McCulloh, T.H. (eds.) *Thermal history of sedimentary basins. Methods and case histories*. Springer, New York, (1989).

Singh, R., Kanwar, S.S., Jaggi, G.S. and Kartha, K.N.K. (2004). Geochemistry of thermal springs from Bhutan Himalaya. *Journal of the Geological Society of India, 64,* 191-198.

WHO Guidelines for drinking-water quality: fourth edition incorporating the first and second addenda. World Health Organization, (2022). 583 pp.

Table A1. *Results of chemical analysis on representative water samples from hot springs from nine geothermal areas in Bhutan, and one sample of river water. Concentrations are given as mg/L.*

Location	Chubu Tshachu 1	Duenmang Tshachu 2	Gasa Tshachu	Gayza Tshachu 1	Gelephu Tshachu 1	Khambalung Ney Tshachu 2	Koma Tshachu 1	Phedey Tshachu 1	Yoeten Kuenjung Tshachu	Mo Chu River
Date	2024-05-14	2024-06-18	2024-04-30	2024-10-18	2024-05-01	2024-11-06	2024-05-14	2024-11-20	2024-11-06	2024-04-30
Flowrate [L/s]	1.1	0.60	~25	0.28	0.17	2.5	0.15	0.2	-	-
Temperature [°C]	48.8	53.0	43.1	39.5	39.3	41.4	40.0	28.8	39.1	9.5
pH - field [pH / °C]	9.19 / 48.8	7.39 / 53.0	6.82 / 40.5	7.68 / 39.5	7.35 / 39.3	9.85 / 41.4	9.96 / 40.0	9.42 / 28.8	9.91 / 39.1	8.03 / 9.5
pH - lab [pH / °C]	8.33 / 23.0	7.57 / 21.7	6.87 / 22.9	6.66 / 22.7	7.23 / 23.1	9.33 / 22.2	9.06 / 22.7	9.62 / 22.6	9.47 / 22.0	-
EC at 25°C [µS/cm]	583	544	8790	1820	839	197	405	1760	234	72.1
DIC (as CO_2)	115	105	2160	971	139	18.5	61.0	4.6	25.4	-
Boron (B)	1.40	0.0934	75.3	5.50	0.331	0.0654	0.679	0.515	0.155	0.094
Silica (SiO_2)	57.3	30.3	115	105	24.2	36.0	44.0	28.7	43.7	5.00
Sodium (Na)	120	20.2	2020	399	74.7	28.9	78.6	222	40.2	1.99
Potassium (K)	2.18	11.2	187	15.0	20.8	0.651	0.738	3.94	0.870	0.498
Magnesium (Mg)	0.0926	8.28	27.7	1.87	11.4	0.0720	0.0692	0.118	0.108	1.19
Calcium (Ca)	2.78	76.0	111	37.7	82.8	6.70	2.36	216	18.4	10.2
Fluoride (F)	14.5	0.221	4.23	7.66	0.689	2.92	17.4	6.07	5.19	0.225
Chloride (Cl)	60.0	4.49	1820	117	9.64	3.94	29.1	17.8	6.18	0.547
Bromide (Br)	0.223	0.046	9.45	0.381	0.027	<0.02	0.105	0.040	0.030	<0.01
Nitrate (NO_3)	<0.1	0.21	<0.1	0.06	<0.1	0.11	0.49	0.18	<0.02	0.93
Sulphate (SO_4)	26.1	147	65.7	55.2	269	41.4	20.5	897	38.8	6.18
Aluminium (Al)	0.0404	0.00555	0.00411	0.00463	0.00418	0.0405	0.0465	0.0338	0.0381	0.0216
Arsenic (As)	<0.00005	0.00152	0.467	0.110	<0.00005	0.00530	<0.00005	<0.00005	0.0109	<0.01
Barium (Ba)	0.000731	0.0602	0.533	0.0645	0.0382	0.000268	0.000196	0.00688	0.00304	0.00128
Chromium (Cr)	0.0000286	0.0000533	0.000114	<0.00001	0.0000585	0.0000128	0.0000163	0.000100	0.0000365	<0.007
Copper (Cu)	0.000200	0.000166	0.000463	0.000157	<0.0001	<0.0001	0.000188	0.000230	0.000161	<0.01
Iron (Fe)	0.0512	0.00139	0.451	0.0152	0.0294	0.000730	0.00366	0.00754	0.00374	0.00320
Lithium (Li)	0.0607	0.0343	7.91	0.674	0.104	0.0217	0.0265	0.0501	0.0578	0.00313
Manganese (Mn)	0.00585	0.0000750	0.0709	0.201	0.0430	0.0000698	0.000592	0.00138	0.00121	<0.0009
Molybdenum (Mo)	0.00288	0.00434	0.000201	0.000600	0.000368	0.00380	0.00502	0.00268	0.00555	<0.02
Nickel (Ni)	<0.00005	0.0000712	0.000142	0.0000548	0.0000766	<0.00005	<0.00005	<0.00005	0.0000585	<0.001
Lead (Pb)	0.0000302	0.0000222	0.0000352	<0.00001	<0.00001	0.0000329	0.0000472	0.000358	0.0000937	-
Strontium (Sr)	0.0251	1.55	1.78	0.790	5.11	0.0822	0.00848	0.957	0.0639	0.0196
Zinc (Zn)	0.00110	0.00292	0.0359	0.00223	<0.0002	0.0177	0.00190	0.0173	0.00825	<0.003
Diss. solids (TDS)	359	330	5420	1210	571	129	217	1390	141	-
δD [‰SMOW]	-104.78	-58.41	-92.30	-120.44	-50.84	-85.48	-96.66	-57.91	-89.75	-64.68
$\delta^{18}O$ [‰SMOW]	-14.14	-7.90	-11.16	-16.37	-7.98	-12.74	-12.30	-8.69	-13.28	-10.08